Determination of the In-Flight Spectral and Radiometric Characteristics of the Airborne Visible/Infrared Imaging Spectrometer (AVIRIS)

Robert O. Green, James E. Conel, Veronique Carrere, Carol J. Bruegge,
Jack S. Margolis, Michael Rast, and Gordon Hoover

Jet Propulsion Laboratory
California Institute of Technology

ABSTRACT

A valid spectral and radiometric calibration of radiance-measuring instruments is required for physically based analysis of the measured data and for quantitative comparison of data acquired from different sites, times, and instruments. AVIRIS is a science-research imaging spectrometer that measures radiance in 224 channels between 400 to 2450 nm in the electromagnetic spectrum. On the 20th of September 1989, a validation and calibration experiment was performed to determine the in-flight spectral and radiometric characteristics of AVIRIS. Five data sets were acquired over a calibration site on the homogeneous playa of Rogers Dry Lake, California. Surface reflectance, atmospheric optical depths, and atmospheric water-vapor measurements were acquired concurrently with the overflights. These in situ measurements were used to constrain the LOWTRAN-7 radiative-transfer code to predict the total spectral radiance incident at the AVIRIS aperture. These predicted radiances and the AVIRIS-measured radiances were analyzed to validate the in-flight characteristics. In-flight spectral channel positions and response functions over the AVIRIS spectral range were derived. Radiometric calibration coefficients were calculated for channel as well as radiometric accuracy, intraflight stability, and noise-equivalent delta radiance. These analyses both validate the laboratory-based calibration and allow direct generation of a valid spectral and radiometric calibration for AVIRIS inflight.

INTRODUCTION

AVIRIS measures total radiance in 224 spectral channels from 400 to 2450 nm in the electromagnetic spectrum. The sampling interval and spectral response function for full width at half maximum (FWHM) is nominally 10 nm over this spectral range. As an example of the spectral and radiometric properties of AVIRIS data, Figure 1 presents a high-spectral-resolution LOWTRAN-7 (Kneizys et al., 1989) spectrum for a surface of 50-percent reflectance at sea level under a 23-km midlatitude summer atmospheric model with a 23.5-degree solar zenith angle. The 10-nm spectral channels used to convolve the high-resolution spectrum to the AVIRIS spectral characteristics and the resulting modeled AVIRIS spectrum are also shown.

AVIRIS data are acquired at a flight altitude of 20 km and at a rate of 7300 spectra per second. The spatial resolution is nominally 20 by 20 m with an image area of 10.5 by up to 100 km. Spectral and radiometric properties of AVIRIS are determined in the laboratory (Chrien et al., 1990) preceding and following each period of operation.

To verify the accuracy of this laboratory calibration, an in-flight validation and calibration experiment was held on the 20th of September 1989 at Rogers Dry Lake, California. This site was selected for the homogeneity of the surface at the AVIRIS spatial scale, the access to radiosonde data acquired regularly at a nearby air force base, and the facilities available for supporting surface and atmospheric measurements. Rogers Dry Lake is located in the Mojave desert approximately 100 km north of Los Angeles, California. Measurements of the surface reflectance, the atmospheric optical depths, and atmospheric

water vapor were acquired concurrently with the AVIRIS overflights. These surface-based measurements were used in conjunction with the LOWTRAN-7 radiative-transfer code to predict at high resolution the total spectral radiance incident at AVIRIS. Through analyses with these modeled radiances and the actual measured radiances, the in-flight spectral-channel positions and spectral-response functions FWHM were determined. With these data, the radiometric accuracy, the intraflight stability, and the noise-equivalent delta radiance (NEdL) were calculated. These in-flight determinations were compared with the laboratory-derived equivalents to both validate and calibrate the AVIRIS characteristics in flight.

AVIRIS CHARACTERISTICS

AVIRIS spectral and radiometric properties were designed primarily from science investigations with the Airborne Imaging Spectrometer (AIS) and with laboratory spectrometer research. The nominal AVIRIS characteristics are given in Table 1. The spectral range of 400 to 2450 nm corresponds to a region in the electromagnetic spectrum where the atmosphere is largely transmissive. Compositional information is contained within this range for the scientific disciplines of ecology, geology, oceanography, atmospheric studies, and snow and ice hydrology. AVIRIS uses four spectrometers with the following nominal ranges: A (400 to 710 nm), B (670 to 1290 nm), C (1250 to 1870 nm), and D (1830 to 2450 nm). Over the entire range, the AVIRIS spectral-channel sampling intervals and the response functions (FWHM) for the 224 channels are nominally 10 nm. In the laboratory, these spectral properties are determined for each channel to better than 2 nm (Chrien et al., 1990).

Table 1. AVIRIS spectral and radiometric characteristics

Spectral	
Wavelength range	400 to 2450 nm
Channel sampling interval	9 to 12 nm
Channel response function	9 to 12 nm
Sampling-interval calibration	<= 2 nm
Response-function calibration	<= 2 nm
Radiometric	
Radiometric range	0 to maximum lambertian terrestrial radiance
Radiometric digitization	>= 1 DN noise
Absolute calibration	<= 10.0%
Intraflight stability	<= 2.0%
Noise-equivalent delta radiance	approximately meeting spectral requirement

The radiometric range of AVIRIS is defined such that a 100-percent lambertian reflectance surface with a 0-degree solar zenith angle will not saturate the 1024 bits of digitization. Digitization is set to greater than 1 digitized number (DN) of noise within the constraint of the radiometric range requirement. Absolute radiometric, stability, and vignetting calibrations are established in the laboratory.

A radiometric precision requirement for AVIRIS was initially defined through a signal-to-noise requirement for the AVIRIS reference radiance. A spectrum of the reference radiance is given in Figure 1 and the signal-to-noise requirement in Figure 2. Figure 3 gives the corresponding AVIRIS noise-equivalent delta radiance requirement. NEdL is defined for each AVIRIS channel as the reference radiance divided by the signal-to-noise requirement as in Equation 1. NEdL unambiguously reports the precision in AVIRIS-

measured radiance for each spectral channel. To meet this precision requirement, the AVIRIS NEdL must be less than the NEdL requirement at each channel.

$$NEdL_{REQ} = L_{REF} / SNR_{REQ} \quad (1)$$

AVIRIS LABORATORY CALIBRATION

Spectral calibration in the laboratory is carried out by recording the output of a channel as calibrated monochromatic light is scanned across the spectral range of that channel. The resulting normalized curve gives the channel's position and spectral-response function. Nominally, 15 channels are measured in each spectrometer. Spectral characteristics for the entire suite of channels are generated through fitting a second-order polynomial to the measured channels for each spectrometer. The spectral response function of each AVIRIS channel may be accurately modeled by a Gaussian function with the appropriate FWHM. An example of the validity of this approximation is shown in Figure 4 by the agreement between the laboratory-measured response function and the Gaussian-modeled function for channel 150. Distribution of the AVIRIS spectral channels across the spectral range is given in Figure 5. The interpolated spectral response function FWHM for each channel is given in Figure 6. These spectral properties are not uniform across the spectral range; therefore, an accurate calibration is essential.

The importance of spectral calibration for quantitative analysis of data is shown through the retrieval of surface-reflectance spectra from AVIRIS-measured radiance. Surface reflectance is calculated from measured radiance spectra using a radiative-transfer code through constraint of atmospheric and illumination parameters. Figure 7 presents a calibration sensitivity analysis of the spectral-channel position for the recovery of a 25-percent surface reflectance spectrum from a corresponding modeled LOWTRAN-7 radiance spectrum. The reflectance is retrieved with a 0.1-, 1.0-, and 5.0-nm error in the calibration of the spectral-channel positions. As the error in knowledge of the channel position increases, the sharp features and steep slopes of radiance spectrum cause increasingly large errors in the retrieved reflectance. For the case of a 5.0-nm miscalibration, an error in reflectance of 20 percent results through failed compensation for the 1130-nm atmospheric water band. A similar analysis based on an error in calibration of the channel-spectral-response function is given in Figure 8. In the regions of strong atmospheric absorptions, for example the 760-nm oxygen band, a good spectral-response-function calibration is required to accurately retrieve reflectance from measured radiance. These analyses demonstrate the sensitivity of derived parameters, such as spectral reflectance, to the accuracy of spectral calibration.

AVIRIS is radiometrically calibrated in the laboratory by acquiring a large sample of data over an integrating sphere of known spectral radiance. For each channel, the radiance of the integrating sphere is divided by the mean dark-current-subtracted DN to generate the radiometric calibration coefficients. Figure 9 gives the laboratory-determined coefficients determined for the 20th of September 1989. Vignetting characteristics are generated by determining the change in throughput across the scan for all spectral channels. Vignetting calibration coefficients are calculated as the inverse of the scan-center normalized throughput.

Radiometric stability is determined during the laboratory calibration over a period of several hours of AVIRIS operation. Figure 10 gives the percent deviation from the mean for a set of one minute of AVIRIS data samples acquired every half hour during a 4-hour period following a 1-hour warm-up of AVIRIS and the integrating sphere. AVIRIS is stable at the 1-percent level in the laboratory over most of the spectral range. Lower

apparent stability at the short- and long-wavelength ends of the range are attributable to the extreme low intensity of the integrating sphere radiance in these spectral regions.

Noise is calculated as the root-mean-squared deviation (RMSD) of a sample of 100 spectra measured from the stabilized integrating-sphere radiance source. An equally valid method for calculating the noise is to form the RMSD of 100 samples of AVIRIS dark-current data, which represent a stable dark source. Figure 11 gives the noise calculated using both of these methods.

Radiometric precision or NEdL is calculated by multiplying the DN noise by the radiometric calibration coefficients. This NEdL is the precision-based uncertainty for AVIRIS-measured radiance. Figure 12 gives the NEdL calculated in the laboratory as a function of wavelength and is compared to the AVIRIS requirement. This graph shows AVIRIS to have greater precision than required over most of the spectral range.

IN-FLIGHT CALIBRATION EXPERIMENT MEASUREMENTS

To validate the laboratory calibration of AVIRIS data acquired in flight, a reflectance-based calibration experiment was performed at Rogers Dry Lake, California. A homogeneous calibration site of 200 by 20 meters, corresponding to a line of 10 AVIRIS spatial samples, was located and marked on the playa surface with large dark tarps. Surface reflectance of this site across the AVIRIS spectral range was measured at the time of the AVIRIS overflights. The field spectrometer used has a spectral-interval-sampling and response function of less than 5 nm and an approximate 10-cm circular field of view at 1 m. The mean spectral reflectance of the 80 measurements acquired bounded by the RMSD is given in Figure 13.

At a site adjacent to the playa, atmospheric measurements were acquired concurrently with the AVIRIS overflights. A stable solar radiometer with 10 discrete channels with nominal 10-nm spectral-response functions, FWHM, was used to measure solar illumination through the atmosphere. These data were acquired from sunrise to local solar noon on the day of the experiment. Using the Langley plot method (Bruegge, 1985), these data were reduced to atmospheric optical depths. The spectral-channel positions and calculated optical depths are given in Table 2. Vertical-column water vapor was calculated directly from the solar radiometer measurements using the 940-nm channel (Reagan et al., 1987 and Bruegge et al., 1990). A value of 6 mm of precipitable water vapor was derived for the time of AVIRIS overflights. This value agreed with a continuum-interpolated-band-ratio estimate derived directly from the AVIRIS radiance data. This water-vapor retrieval algorithm is described by Green, et al., 1989.

Table 2. Channel positions and derived optical depths from the solar radiometer

20 September 1989, Rogers Dry Lake, California

Channel No.	1	2	3	4	5	6	7	8	9	10
Position (nm)	370	400	440	520	610	670	780	870	940	1030
Optical Depth	.539	.398	.288	.174	.128	.082	.049	.046	.284	.028

PREDICTED AVIRIS RADIANCE

AVIRIS overpasses of the calibration site occurred at 18:28, 18:44, 18:59, 19:14, and 19:29 universal coordinated time (UCT). A LOWTRAN-7 model was used to compute the total incident radiance at the AVIRIS aperture for each overpass. These calculations were constrained by the surface reflectance, optical depth, and water vapor measured at the time the AVIRIS data were acquired. The LOWTRAN-7 code was run at the highest spectral sampling interval, which is better than that of AVIRIS in the range of 400 to 2450 nm. Model spectra were convolved to the AVIRIS spectral-sampling intervals and response function measured in the laboratory. These five LOWTRAN-7 total spectral-radiance curves are shown in Figure 14. The increase in radiance for consecutive spectra results from the decrease in the solar zenith angle as the overpass times approach local solar noon.

REPORTED AVIRIS RADIANCE

AVIRIS data acquired over the Rogers Dry Lake calibration site were calibrated to radiance by application of the laboratory calibration coefficients. The calibrated data acquired over the calibration site at Rogers Dry Lake on the 20th of September 1989 are shown in Figure 15. Excellent agreement is observed between the LOWTRAN-7-predicted and the AVIRIS-measured spectral radiances.

SPECTRAL VALIDATION AND CALIBRATION

Validation of the in-flight spectral properties of AVIRIS is based on a least-squared-error minimization algorithm operating on the high-spectral-resolution LOWTRAN-7-modeled radiance and the AVIRIS-measured radiance. The algorithm begins with a modeled high-resolution spectrum for an atmospheric absorption band and the corresponding AVIRIS-measured radiance spectrum. A least-squared-error fit is derived for the in-flight spectral characteristic that results in the best agreement between the LOWTRAN-7-modeled and AVIRIS-measured spectrum. An in-flight spectral-channel-position and response-function FWHM is returned for each atmospheric absorption band examined. This approach to in-flight spectral calibration was initially implemented graphically for AIS (Conel et al., 1987); an improved computational procedure was implemented for AVIRIS data (Green et al., 1988).

The root-mean-squared-error calculations fitting the 940-nm atmospheric water band for spectral-sampling-interval and response-function FWHM are shown in Figures 16 and 17. The in-flight spectral-sampling interval is best fit with a 0.5-nm channel shift to shorter wavelengths relative to the laboratory calibration. The in-flight spectral-response FWHM is optimized with a 0.4-nm broadening of the response function measured in the laboratory. Figure 18 shows the resulting fit between AVIRIS and LOWTRAN-7 spectra for this atmospheric-absorption band.

This algorithm was applied to 10 atmospheric absorption bands across the AVIRIS spectral range. In Table 3, the results of this validation are given as the deviation of the laboratory-calculated spectral-channel positions and response functions from the in-flight-determined spectral characteristics.. Atmospheric-absorption bands were examined in each of the four AVIRIS spectrometers. For these bands, the laboratory channel-position calibration is shown to be valid to within 2 nm. The spectral-response functions determined in the laboratory also agree with those determined in flight at the 2-nm level, with exception of the 1130-nm water band. The anomalous result for this band is attributed to a discrepancy in the laboratory radiometric calibration in this spectral region and not to an actual broadening of the response function (Chrien et al., 1990). With the determination of the spectral-channel-sampling interval and response function at points across the AVIRIS

spectral range, a complete in-flight spectral calibration may be generated by fitting functions to these data over the range of each spectrometer.

Table 3. Spectral-validation results for atmospheric-absorption bands in each of the AVIRIS spectrometers. Deviation of the laboratory spectral-channel position and response function is given with respect to the in-flight determination.

20 September 1989, Rogers Dry Lake, California

AVIRIS SPECTROMETER	BAND	POSTION (nm)	POSITION (nm) DEVIATION	RESPONSE (nm) DEVIATION
A	H2O	695	+0.5	-0.5
B	H2O	725	+1.0	-0.3
B	O2	765	+0.5	+0.0
B	H2O	940	+0.5	+0.4
B	H2O	1130	+0.0	+5.9
B	O2	1265	-1.0	+0.0
C	CO2	1570	+0.0	-0.7
C	CO2	1605	+1.0	-0.7
D	CO2	2005	+0.0	-1.9
D	CO2	2055	-2.0	-1.8

RADIOMETRIC VALIDATION AND CALIBRATION

An estimate of the accuracy of the radiometric calibration is derived through a comparison of the AVIRIS radiance spectrum and the LOWTRAN-7 predicted radiance for the calibration site, accepting the LOWTRAN-7 radiance as the standard of comparison. The percent deviation of the AVIRIS-measured spectrum from the LOWTRAN-7-modeled spectrum is given in Figure 19. Across the spectral range, with exception of the regions of strong atmospheric water absorption at 1400, 1900, and 2500 nm, AVIRIS agrees to within 10% of the LOWTRAN-7 model. Disagreement in the 1100-nm regions is attributed to an error in the laboratory determination of the integrating-sphere radiance. An improved method for integrating-sphere calibration has been implemented in 1990 (Chrien et al., 1990). For data acquired in 1990, the modified onboard calibrator should provide information for a further improvement in the absolute radiometric calibration of AVIRIS. Investigations of the accuracy of LOWTRAN-7 and other radiative-transfer codes are also essential for improved validation of the in-flight accuracy of imaging spectrometer radiance spectra.

Through a ratio of the LOWTRAN-7 predicted radiance to the AVIRIS DN with dark current subtracted, the in-flight radiometric calibration coefficients were generated for each channel. These are shown in Figure 20. These radiometric calibration coefficients agree at the 10% level with those measured in the laboratory.

To establish the radiometric stability of AVIRIS in flight, variation in the measured radiance data from the five overpasses of the calibration site was analyzed. LOWTRAN-7 radiance spectra were used to normalize the data for the differing illumination and

atmospheric parameters resulting from the different times of data acquisition. The RMSD of the five AVIRIS spectra was calculated as an estimate of the variation and divided by the mean of the spectra. This provides an estimate of the intraflight radiometric uncertainty and is given in Figure 21. For the 1.5-hour period over which the data were acquired, AVIRIS was stable at the level of 2%.

In-flight NEdL was calculated as the product of the DN noise and the radiometric calibration coefficients. In-flight noise for AVIRIS is calculated both as the RMSD of the data over the homogeneous calibration site and as the RMSD of the dark-current values measured at the end of each AVIRIS image line. Noise estimates calculated by these methods are given in Figure 22. Calculation of in-flight noise from the end-of-line dark-current measurements offers a method of determining the AVIRIS noise without the presence of a large homogeneous ground target; this method avoids the influences of inhomogeneous target reflectance and atmosphere. The NEdL for this calibration experiment is given in Figure 23 along with the NEdL requirement. As in the laboratory, AVIRIS is meeting the requirement over most of the spectral range from 400 to 2450 nm.

CONCLUSION

Through an in-flight calibration experiment at Rogers Dry Lake, California, on the 20th of September 1989, the spectral and radiometric properties of AVIRIS were determined. In-flight spectral-channel positions and spectral-response functions in 10 regions of the AVIRIS spectral range, encompassing all four spectrometers, are shown to agree closely with the corresponding parameters measured in the laboratory. These results provide the basis for direct generation of an in-flight spectral calibration of AVIRIS. The radiometric calibration coefficients determined in the laboratory agree to better than 10% with the in-flight determination over most of the spectral range. Greater disagreement occurs in spectral regions of low atmospheric transmittance. The intraflight stability for the Rogers Dry Lake calibration site is better than 2% with exception of the strong atmospheric water absorptions, where the measured radiance is close to zero. This result is consistent with the laboratory determination of stability over several hours. A NEdL determination for the in-flight calibration corresponds closely to the laboratory calculation. This experiment has provided both validation of the laboratory calibration and direct generation of calibration parameters for the in-flight spectral and radiometric characteristics.

ACKNOWLEDGEMENTS

This research was carried out at the Jet Propulsion Laboratory, California Institute of Technology, under contract with the National Aeronautics and Space Administration. Thanks to Bill Tibbitts for his ongoing and extraordinary logistical support at Rogers Dry Lake, California.

REFERENCES

Bruegge, C.J., *In-Flight Absolute Radiometric Calibration of the Landsat Thematic Mapper* (Published under Kastner), Ph.D. Dissertation, University of Arizona, 1985.

Bruegge, C.J., J.E. Conel, J.S. Margolis, R.O. Green, G. Toon, V. Carrere, R.G. Holm, and G. Hoover, "In-situ atmospheric water-vapor retrieval in support of AVIRIS validation," *SPIE*, Vol. 1298, *Imaging Spectroscopy of the Terrestrial Environment,* 1990.

Chrien, T.G., R.O. Green, and M. Eastwood, "Laboratory spectral and radiometric calibration of the Airborne Visible/Infrared Imaging Spectrometer (AVIRIS)," *SPIE*, Vol. 1298, *Imaging Spectroscopy of the Terrestrial Environment*, 1990.

Conel, J.E., R.O. Green, G. Vane, C.J. Bruegge, and R.E. Alley, "AIS-2 radiometry and a comparison of methods for the recovery of ground reflectance," in *Proceedings of the Third Airborne Imaging Spectrometer Data Analysis Workshop*, G. Vane, Ed., JPL Publication 87-30, Jet Propulsion Laboratory, Pasadena, CA, pp. 18–47 (1987).

Green, R.O., G. Vane, and J.E. Conel, "Determination of aspects of the in-flight spectral, radiometric, spatial and signal-to-noise performance of the Airborne Visible/Infrared Imaging Spectrometer over Mountain Pass, Ca.," in *Proceedings of the Airborne Visible/Infrared Imaging Spectrometer (AVIRIS) Performance Evaluation Workshop*, JPL Publication 88-38, Jet Propulsion Laboratory, Pasadena, CA, pp. 162–184, 1988.

Green, R.O., V. Carrere and J.E. Conel, "Measurement of atmospheric water vapor using the Airborne Visible/Infrared Imaging Spectrometer," ASPRS, *Image Processing '89*, 1989.

Kneizys, F.X., E.P. Shettle, G.P. Anderson, L.W. Abrew, J.H. Chetwynd, J.E.A. Shelby, and W.O. Gallery, *Atmospheric Transmittance/Radiance; Computer Code LOWTRAN 7* (in press), AFGL Hanscom AFB, MA., 1989.

Reagan, J.A., K. Thome, B. Herman, and R. Gall, "Water vapor measurements in the 0.94 micron absorption band: calibration, measurements and data applications," *Proc. IGARSS*, Ann Arbor, pp. 18–21, May 1987.

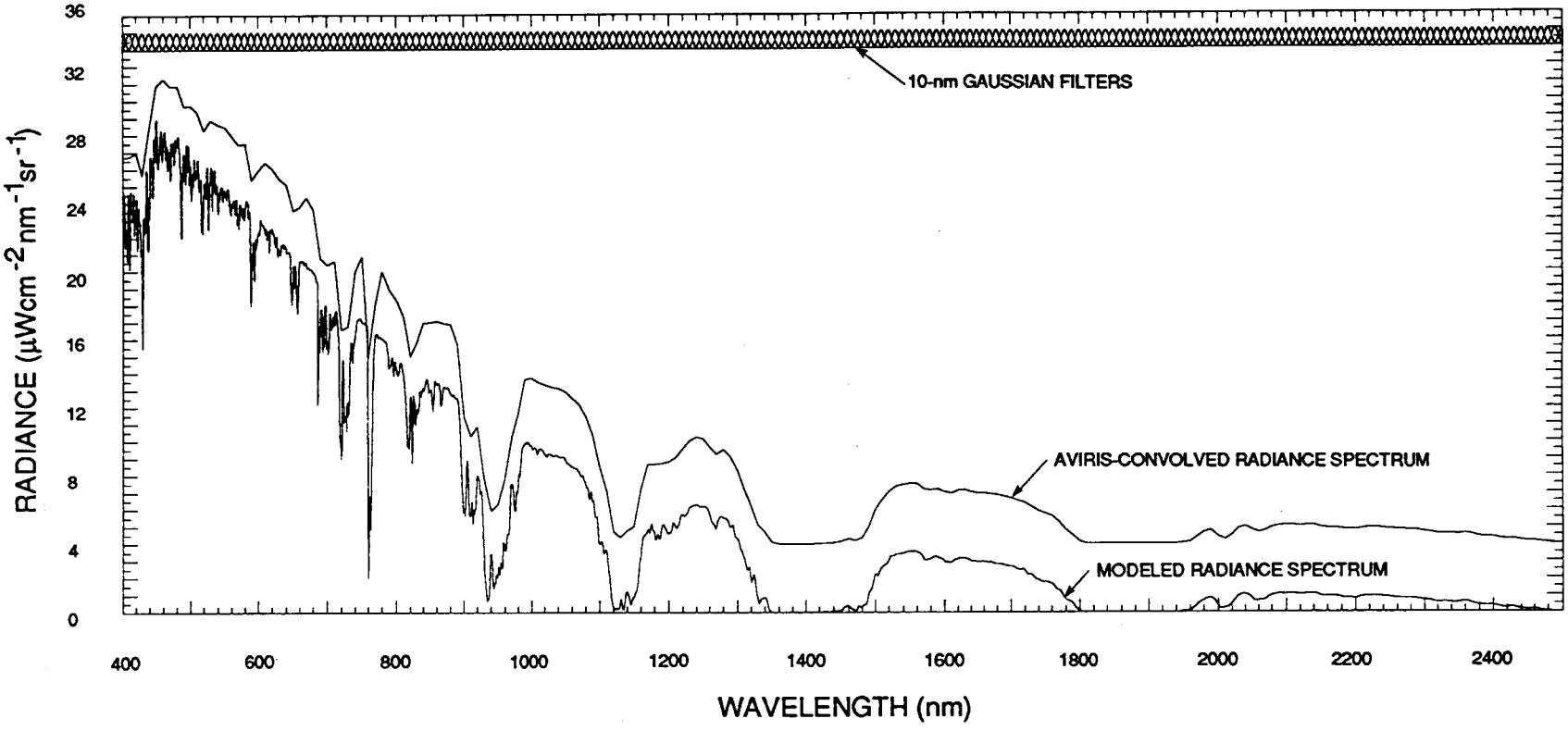

Figure 1. Full-resolution LOWTRAN-7-modeled spectrum, modeled AVIRIS nominal Gaussian filters, and the convolved AVIRIS-modeled spectrum. The AVIRIS spectrum has been offset vertically by 5 radiance units. Constraints on the LOWTRAN-7 model define the AVIRIS reference radiance. The constraints are a 50-percent-reflectance surface, under the 23-km midlatitude summer atmosphere, at local solar noon, on the summer solstice, at 45 degrees north latitude, and at sea level.

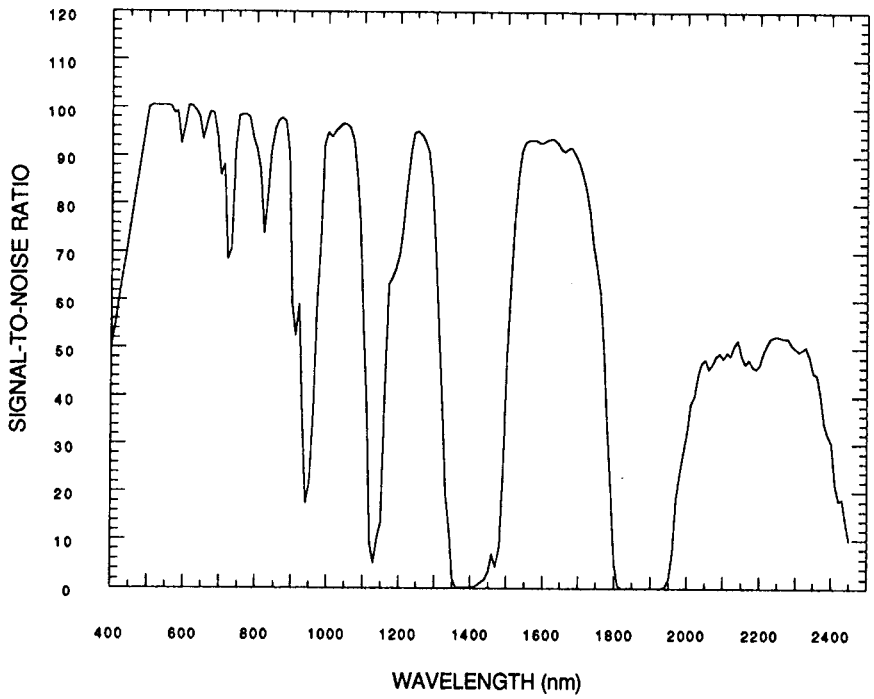

Figure 2. AVIRIS signal-to-noise requirement at the reference radiance level.

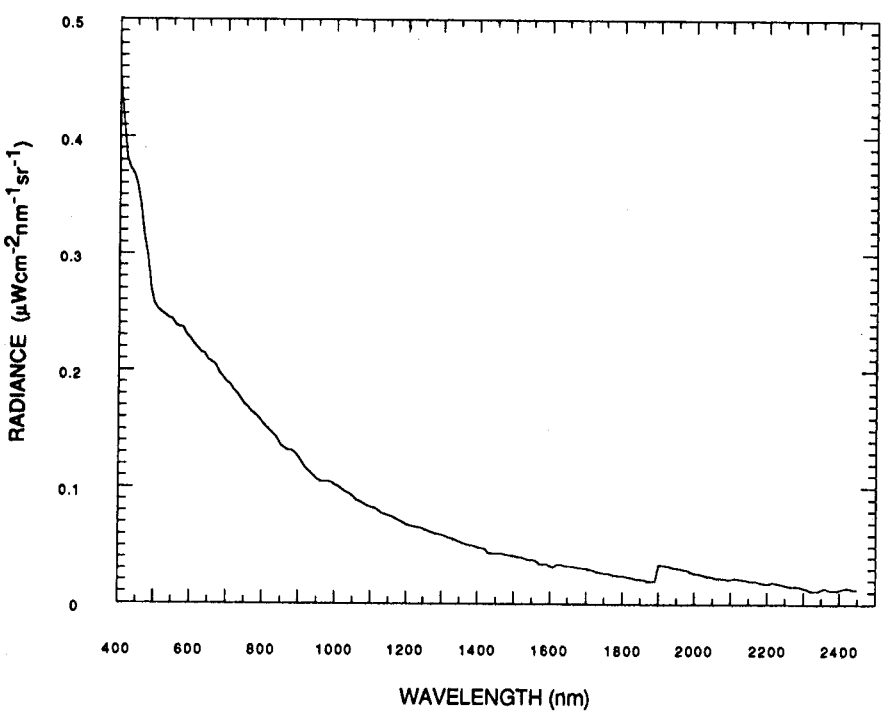

Figure 3. Noise-equivalent delta radiance requirement for AVIRIS calculated as the reference radiance divided by the signal-to-noise requirement.

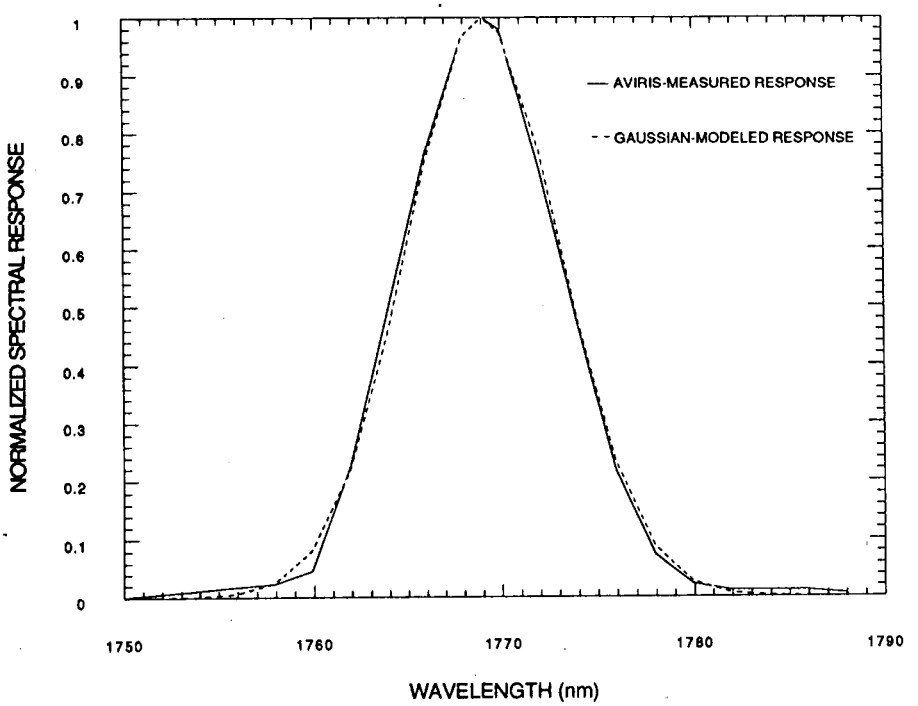

Figure 4. AVIRIS-measured and Gaussian-modeled spectral-response function FWHM for channel 150.

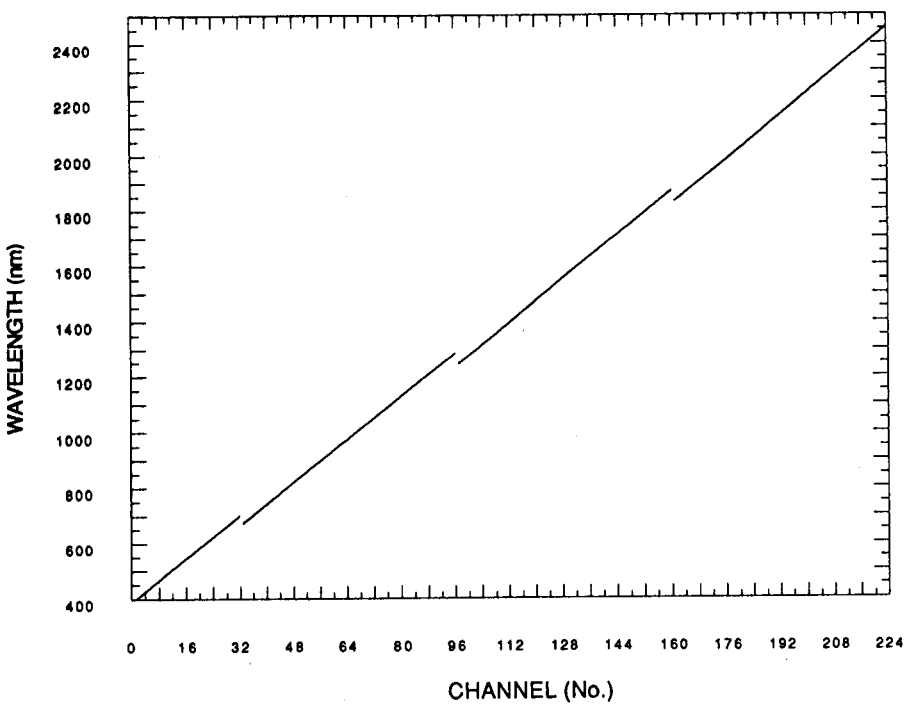

Figure 5. AVIRIS spectral-channel sampling from 400 to 2450 nm.

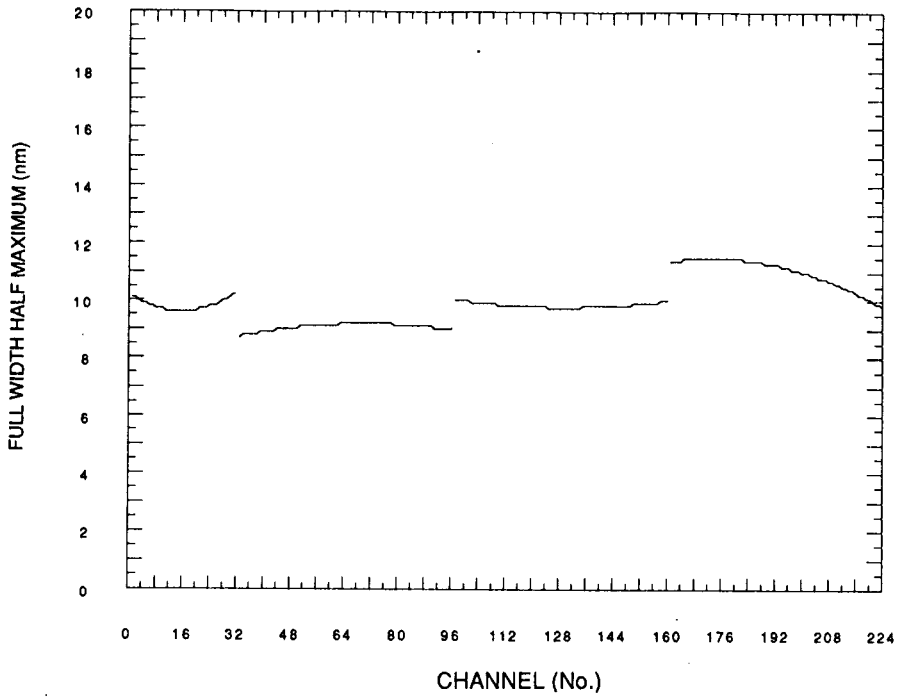

Figure 6. Spectral-channel response functions FWHM for the AVIRIS spectral range.

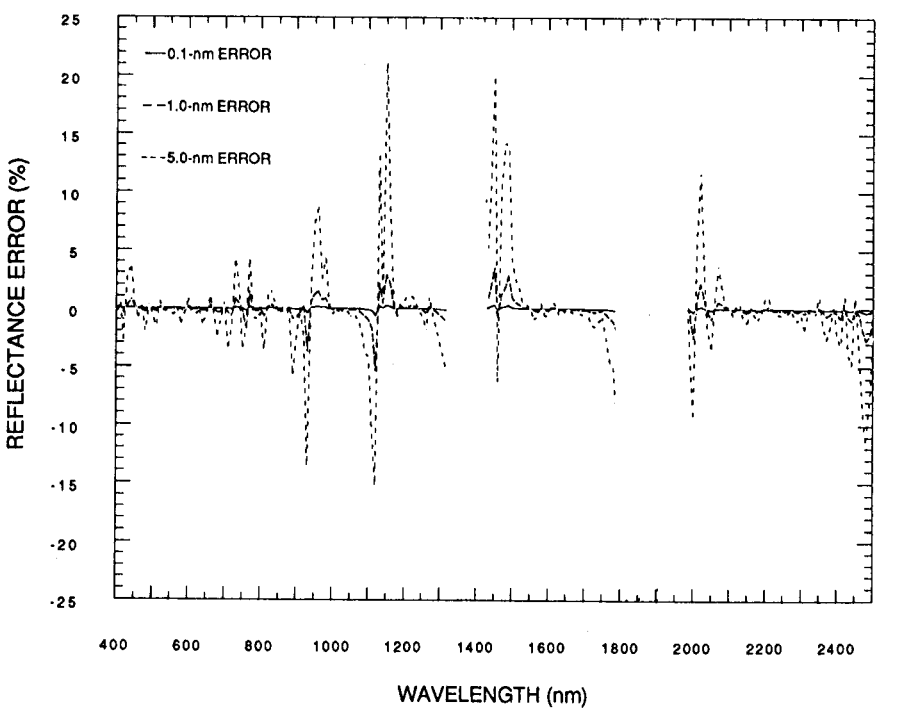

Figure 7. Sensitivity of radiative-transfer-based reflectance retrieval to spectral-channel position calibration. The analysis was based on a LOWTRAN-7 model of a lambertian, horizontal, 25-percent reflectance surface at sea level with the 23-km midlatitude summer atmosphere.

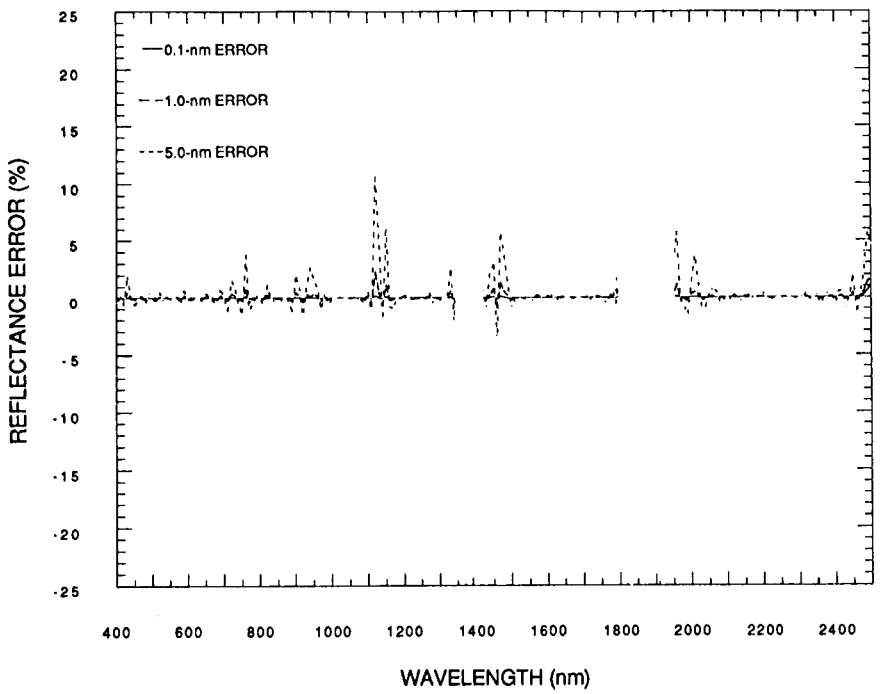

Figure 8. Sensitivity of radiative-transfer-based reflectance recovery to channel-response-function FWHM calibration.

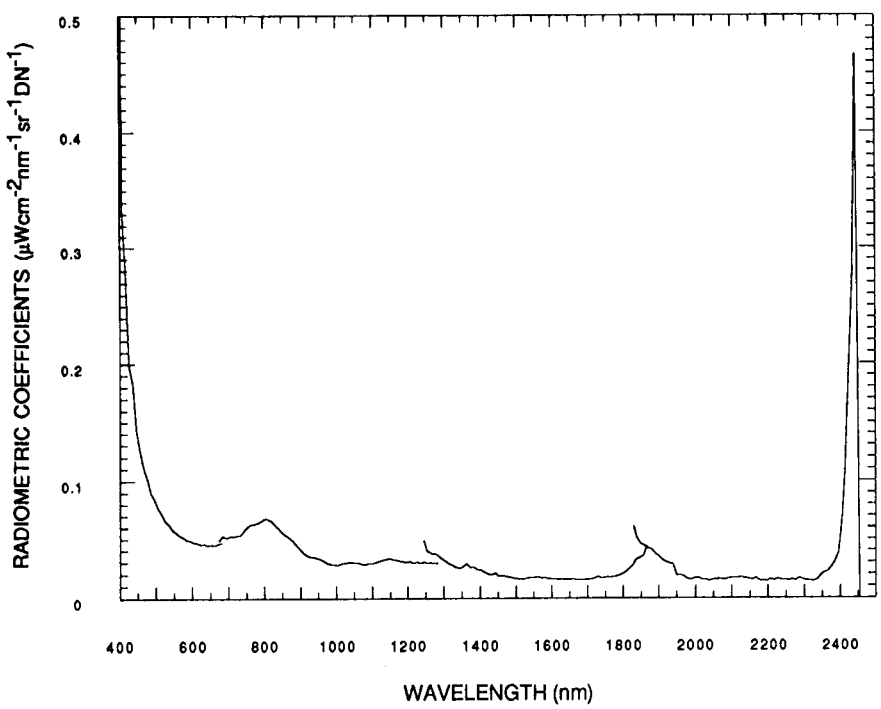

Figure 9. AVIRIS radiometric calibration coefficients determined in the laboratory for the 20th of September 1989 operational period.

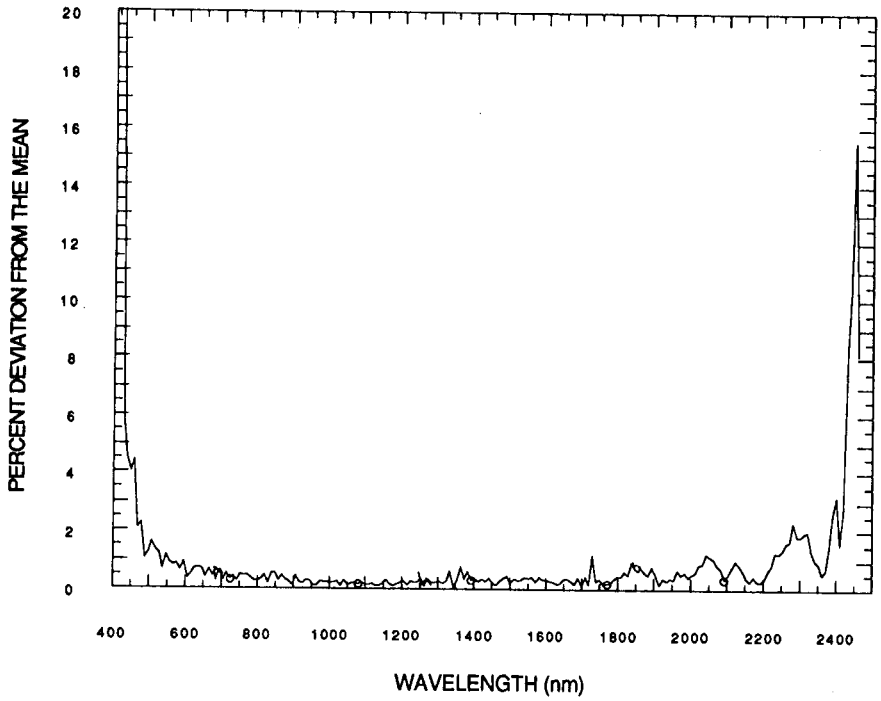

Figure 10. Radiometric stability of AVIRIS over 5 hours during the laboratory calibration.

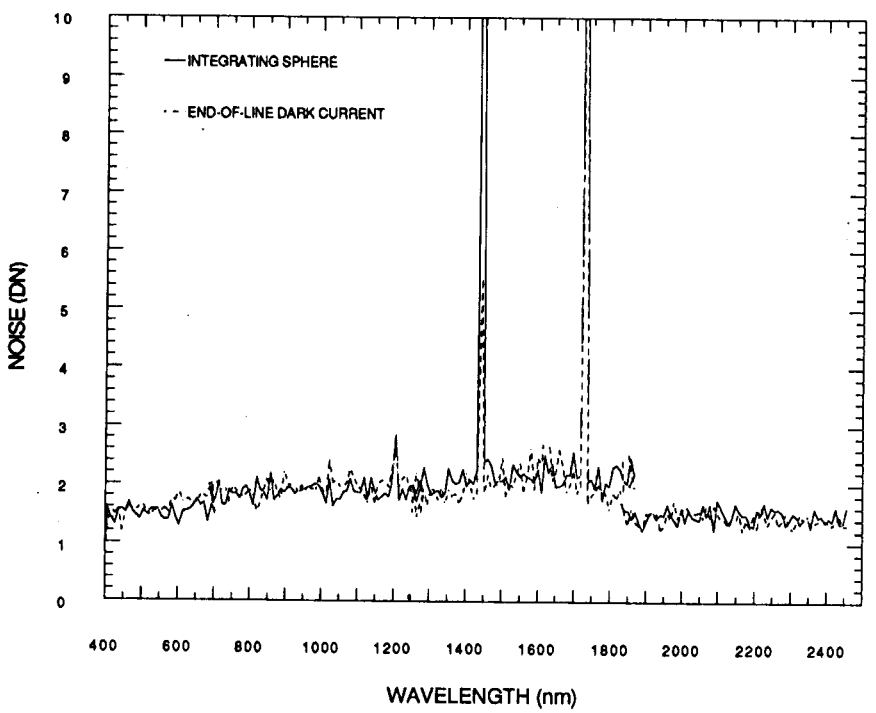

Figure 11. AVIRIS noise calculated both as the RMSD of data acquired over the laboratory integrating sphere and as the RMSD of the dark-current values measured at the end of each AVIRIS image line. In 1989, inherently noisy detector elements were present at 1442 and 1729 nm.

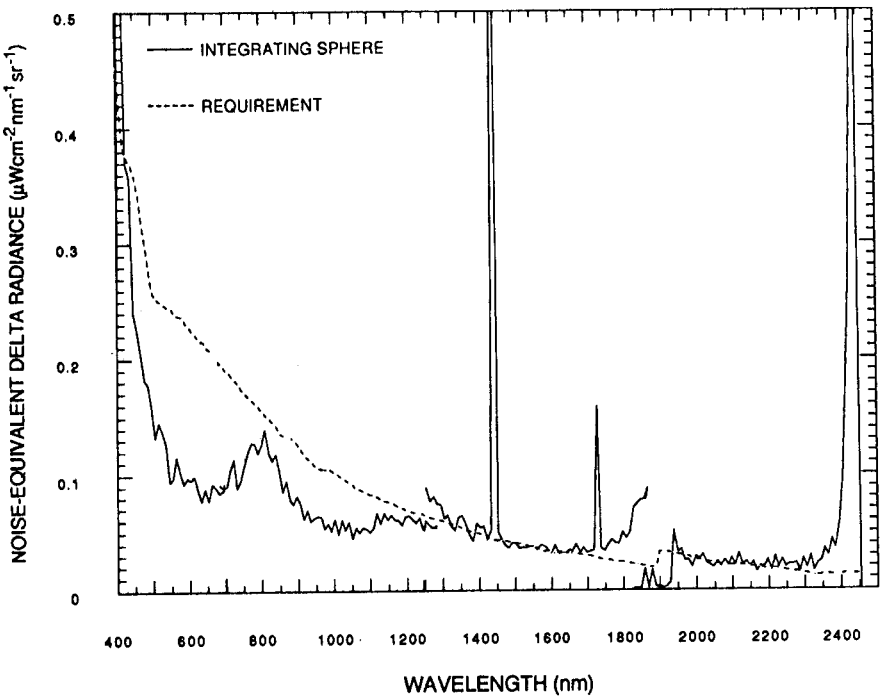

Figure 12. NEdL calculated from laboratory integrating-sphere data for the operational period beginning the 20th of September 1989 and the corresponding requirement. AVIRIS is meeting the NEdL requirement in the laboratory except in the long-wavelength regions of the C and D spectrometers.

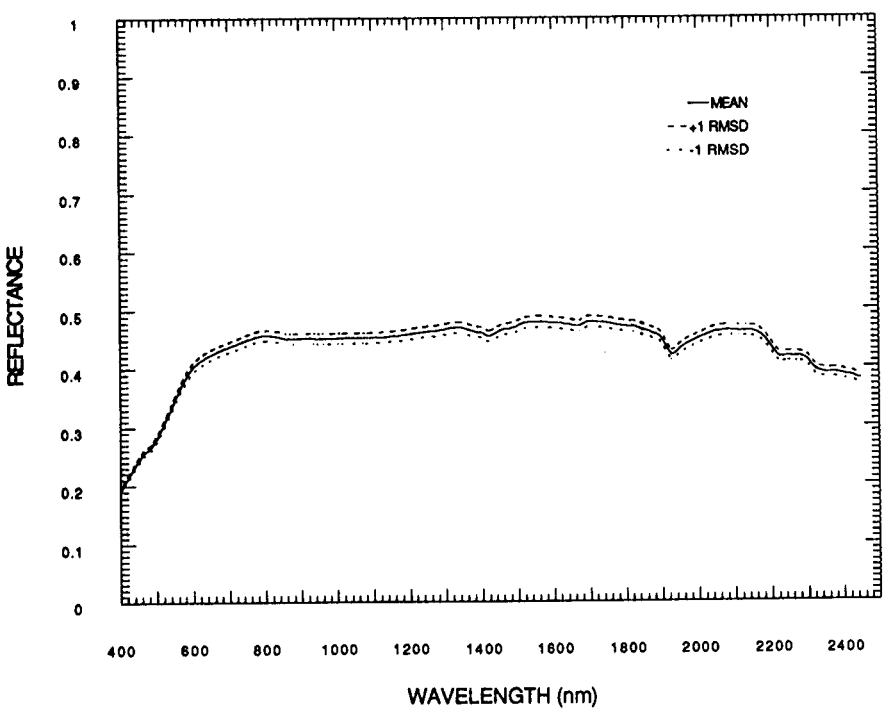

Figure 13. Mean spectral reflectance of 80 measurements of the Rogers Dry Lake calibration site concurrent with the AVIRIS data acquisition. The curve is bounded by the RMSD of these reflectance spectra.

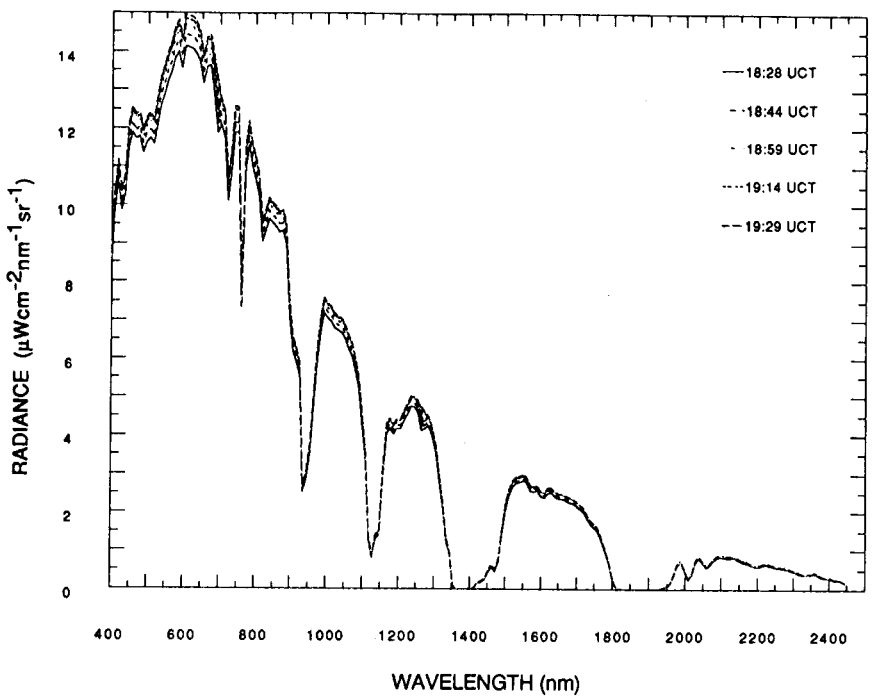

Figure 14. LOWTRAN-7-modeled total spectral radiance for the AVIRIS overflights of the Rogers Dry Lake calibration site on the 20th of September 1989.

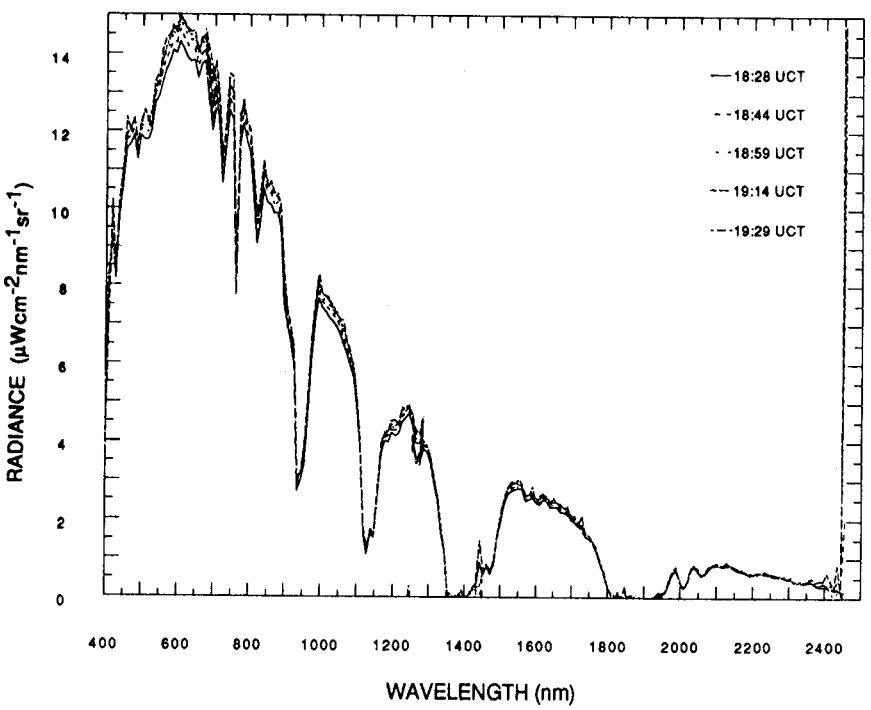

Figure 15. AVIRIS-measured radiance for the five overpasses of the Rogers Dry Lake calibration site.

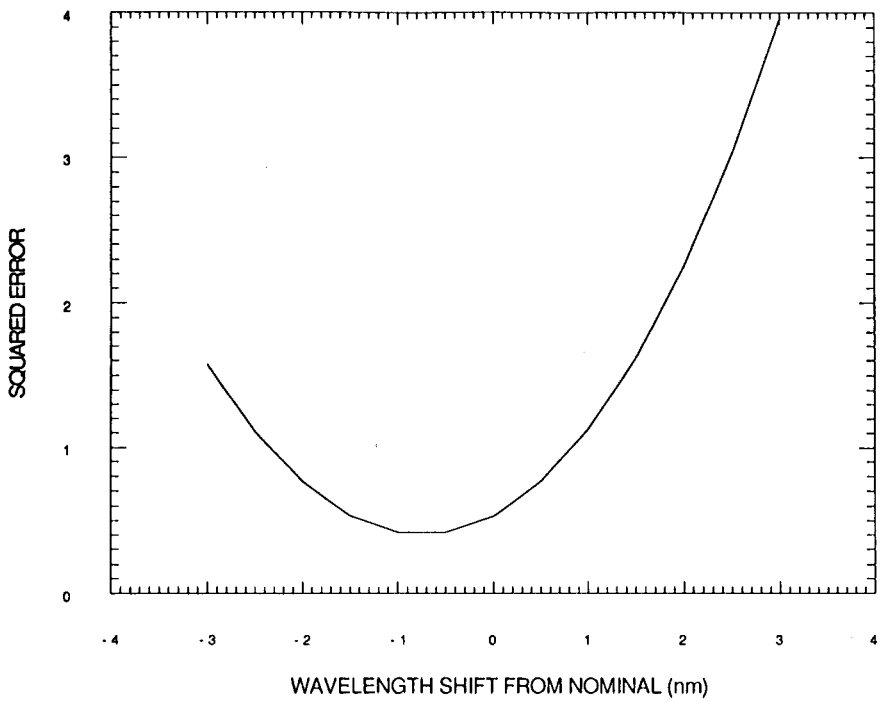

Figure 16. Calibration of spectral-channel position through error minimization between the AVIRIS-measured radiance and the LOWTRAN-7-modeled radiance for the 940-nm atmospheric water band.

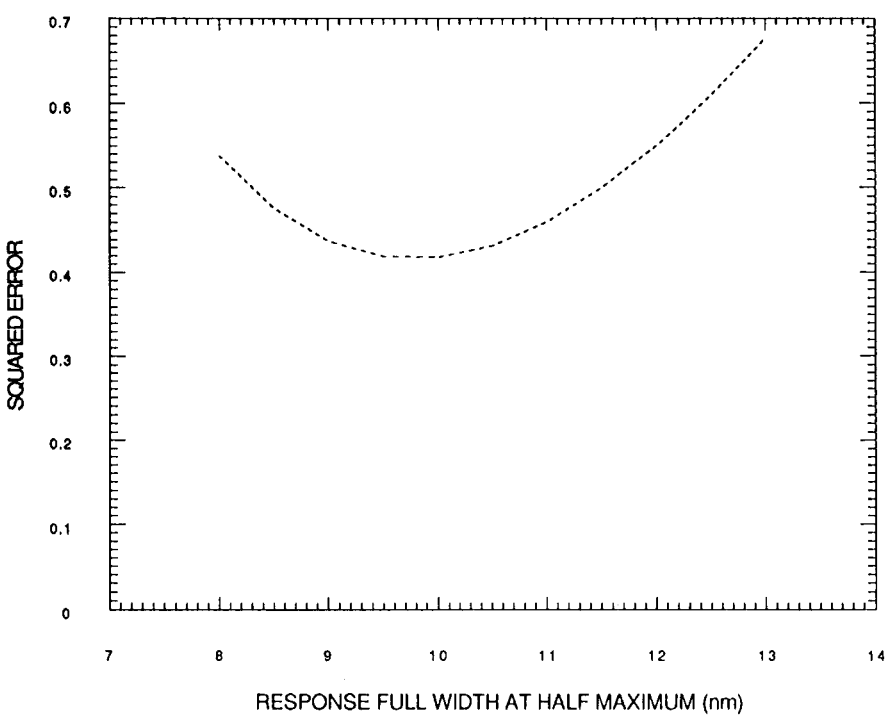

Figure 17. Calibration of spectral-channel-response-function FWHM, through error minimization between the AVIRIS-measured radiance and the LOWTRAN-7-modeled radiance for the 940-nm water band.

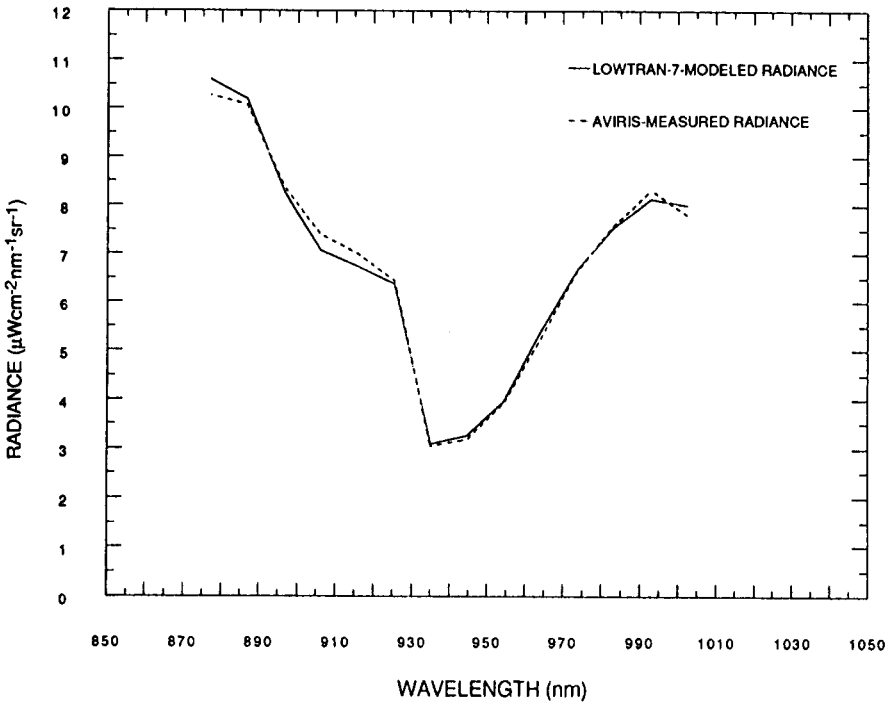

Figure 18. Best-fit result for the AVIRIS in-flight-determined spectral characteristics.

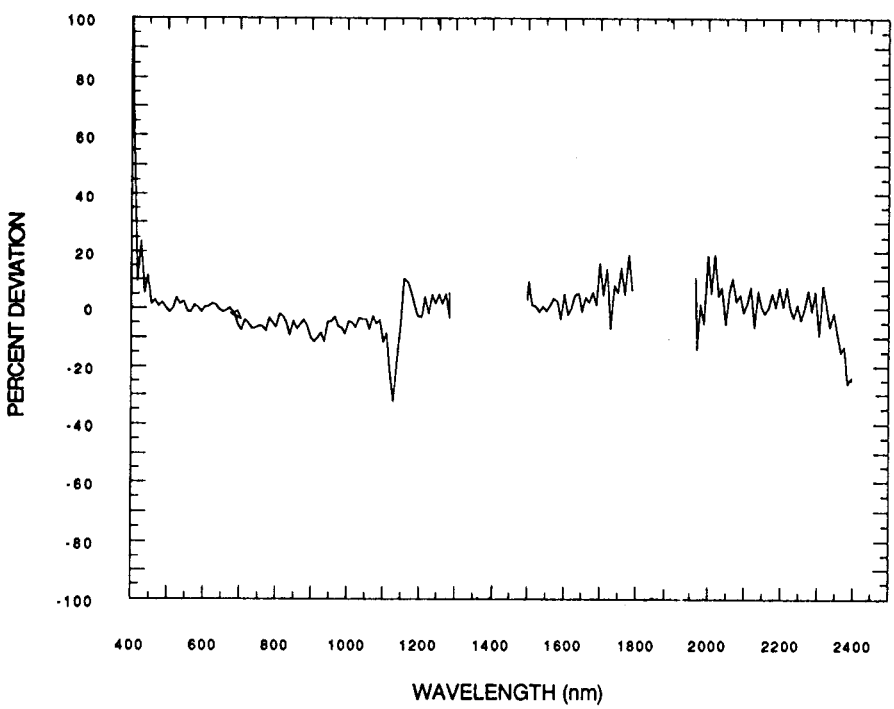

Figure 19. Absolute radiometric accuracy based on the percent deviation of the AVIRIS-measured radiance from the LOWTRAN-7-modeled radiance for the Rogers Dry Lake calibration site on the 20th of September 1989.

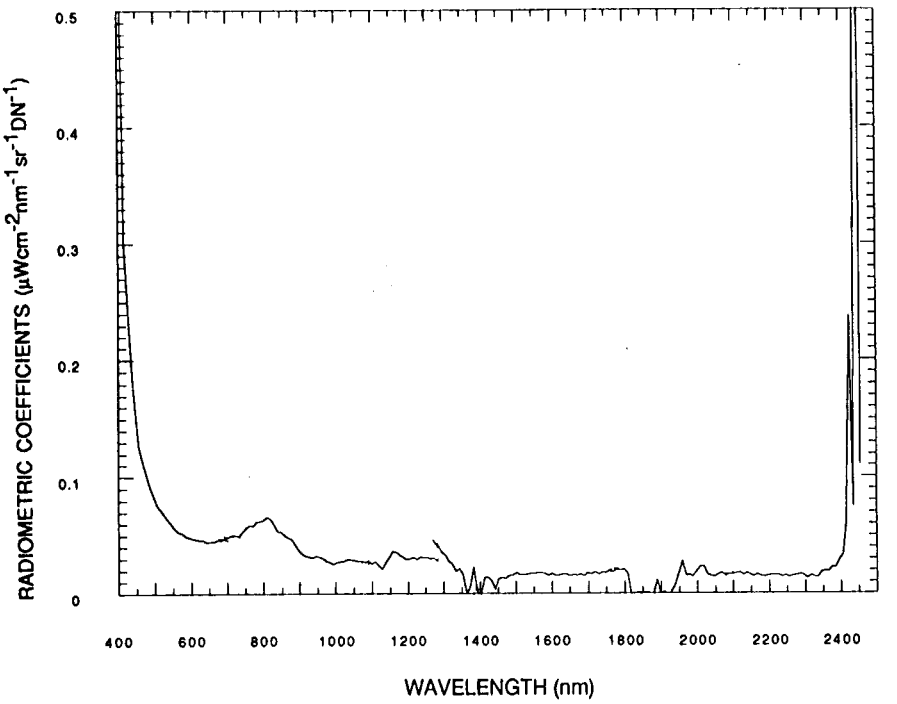

Figure 20. In-flight-determined radiometric calibration coefficients.

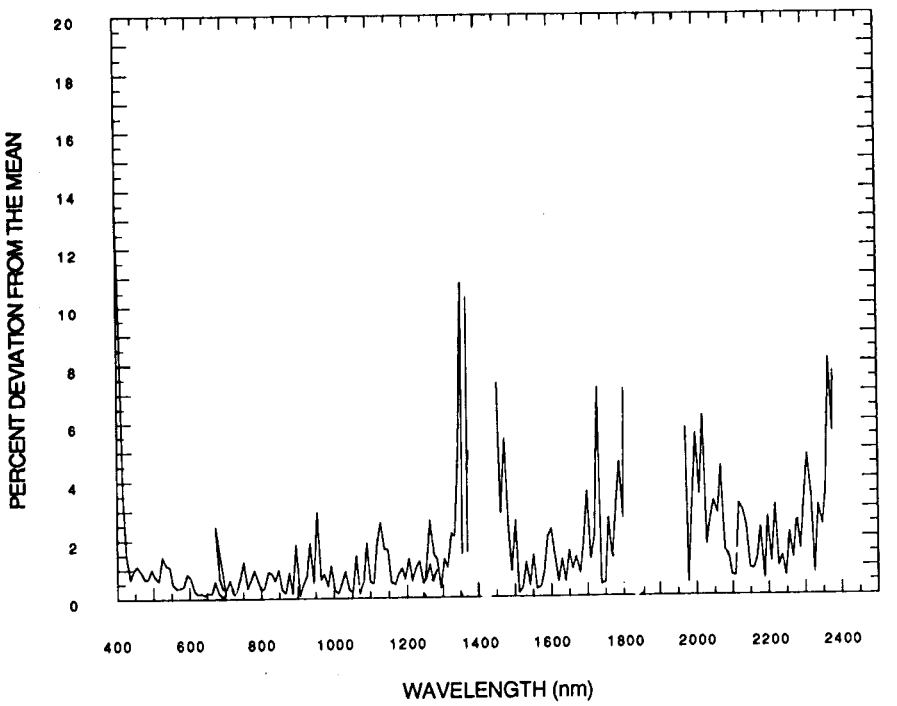

Figure 21. Intraflight radiometric stability based on the percent deviation from the mean of the illumination normalized radiances measured for the five AVIRIS overpasses.

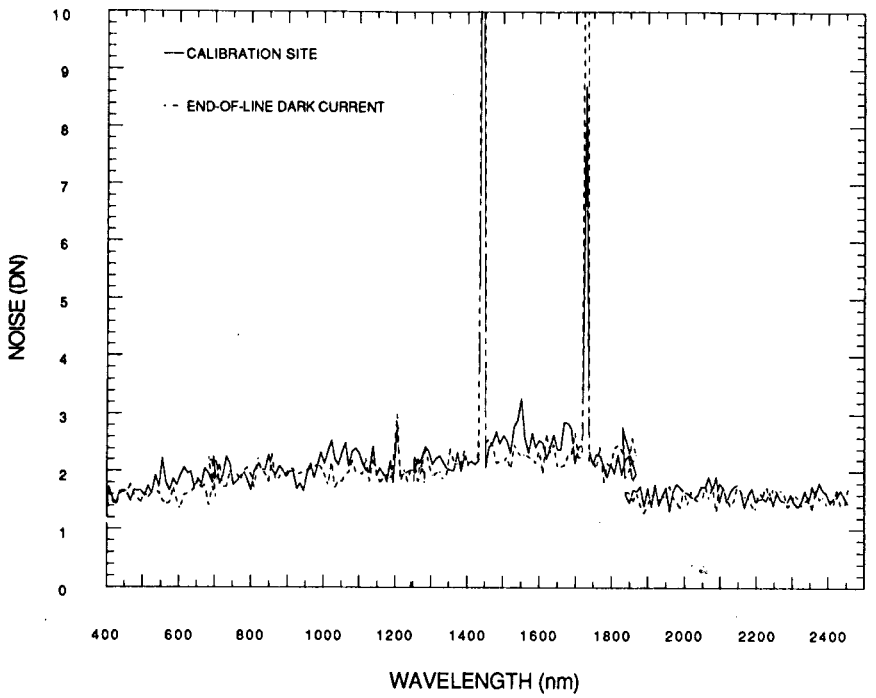

Figure 22. AVIRIS noise calculated from the homogeneous calibration site at Rogers Dry Lake and from the dark-current values measured at the end of each image line.

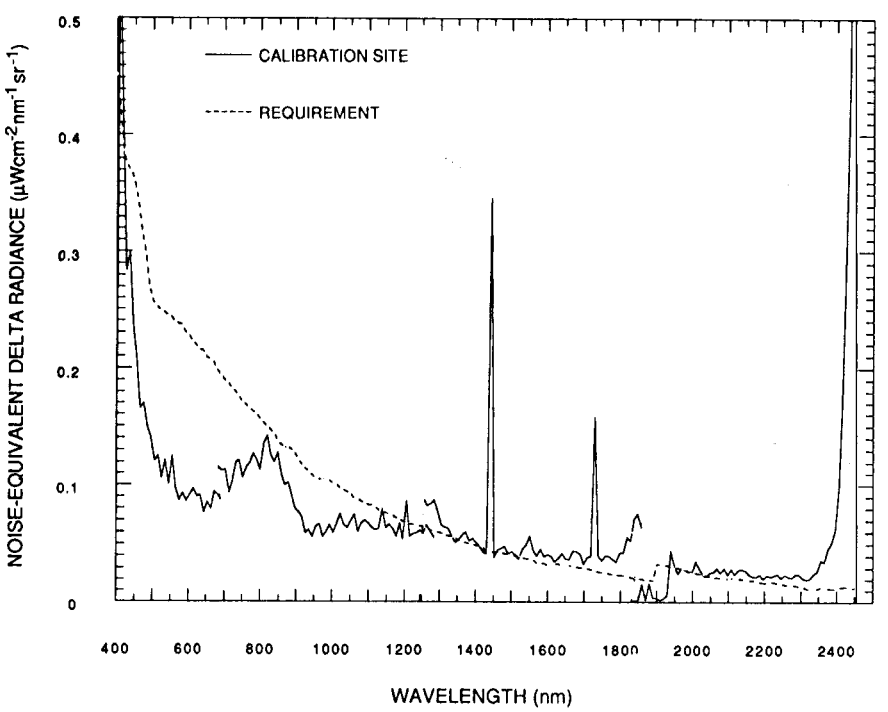

Figure 23. In-flight NEdL determined as the root-mean-squared deviation in the AVIRIS-measured radiance for the homogeneous calibration site at Rogers Dry Lake on the 20th of September 1989.